Mathematical Model for Nitrogen Control in Oxygen Steelmaking

D.A. GOLDSTEIN and R.J. FRUEHAN

A mathematical model was developed to quantify the effects of different operational parameters on the nitrogen content of steel produced during oxygen steelmaking. The model predicts nitrogen removal by the CO produced during decarburization and how the final nitrogen content is affected by different process variables. These variables include the type of coolants used (scrap, direct reduced iron (DRI), *etc.*), the sulfur content of the metal, combined gas blowing practices, and the nitrogen content in the hot metal, scrap and oxygen blown. The model is a mixed control model that incorporates mass transfer and chemical kinetics. It requires a single parameter that reflects the surface area and mass-transfer coefficient that is determined from the rate of decarburization. The model also computes the rate of decarburization and the change in surface active elements, such as sulfur and oxygen, that affect the rate of the nitrogen reaction. Nitrogenization of steel in the converter is also predicted with the model. The computed results are in good agreement with plant data and observations.

I. INTRODUCTION

CONTROL of the nitrogen content of steels during steelmaking has become more important because of the diversity in nitrogen requirements for different steel grades. For example, low carbon sheet steels, intended for special applications such as automobile body panels, require very low nitrogen contents (20 to 50 ppm),[1] whereas tin plate requires high nitrogen levels (60 to 120 ppm).[2] In order to meet these strict specifications, special attention is given to identifying the sources of nitrogen in the steelmaking process and to evaluating possible methods for controlling the nitrogen content of steel. Several investigators have identified the operational factors that affect the nitrogen content of steel produced by electric arc furnace (EAF) and oxygen steelmaking (OSM) processes. These factors are summarized as follows.[3,4,5]

(1) *Carbon oxidation*: Decarburization is one of the most effective ways of reducing the nitrogen content of steel during steelmaking. The CO gas produced during carbon oxidation flushes the nitrogen out of the metal bath and also creates a protective atmosphere over the melt that reduces nitrogen pickup from air.
(2) *Nitrogen content in hot metal*: Hot metal charged into the BOF generally contains 70 to 80 ppm of nitrogen. During decarburization, the nitrogen from the hot metal is removed by the CO gas. Consequently, the final nitrogen content of steel is not strongly affected by the nitrogen present in the hot metal.[3]
(3) *Nitrogen content in scrap*: Scrap is an important source of nitrogen during steelmaking, and its nitrogen content varies from 40 to 220 ppm.[6] Heavy pieces of scrap are difficult to melt and remain unmelted until the end of the blow. At this time, little CO is produced and the nitrogen from scrap remains in the liquid steel produced.
(4) *Direct reduced iron*: Direct reduced iron (DRI) and hot briquetted iron (HBI) generally have lower nitrogen levels than scrap and also melt faster than scrap. Therefore, when DRI products are used as coolants instead of scrap, steels with lower nitrogen contents are produced.[7]
(5) *Oxygen purity*: Nitrogen present as an impurity in the oxygen blown for decarburization can increase the final nitrogen content in the steel produced.[3]
(6) *Combined gas blowing*: The gases used for bottom stirring to improve slag-metal mixing and scrap melting include N_2, Ar, CO_2, O_2, and CO. When nitrogen is used as a stirring gas, it increases the nitrogen content of the steel produced. Therefore, if low nitrogen steels are to be produced, it is necessary to switch from nitrogen to argon in order to avoid excessive nitrogen pickup into the metal.[3]

Other factors that increase the nitrogen content of steel include reblows in oxygen steelmaking, which increases the nitrogen in steel by about 5 to 10 ppm as air is entrained into the furnace.[3] In the EAF, the electric arc also increases the nitrogen content in steel, because it increases the rate of nitrogen pickup into the metal by dissociating the nitrogen molecule.[5,8,9] During tap, nitrogen pickup from air[3] and nitrogen present in alloy additions and carbonaceous materials[5] also increase the final nitrogen content of steel.

In most cases, only qualitative information or empirical data are available on the effects of these process variables on the nitrogen content of the bath. For effective nitrogen control during oxygen steelmaking, quantitative information is required; therefore, a mathematical model that predicts the effects of process parameters on the nitrogen content of the bath needs to be developed. Recently, Kempken and Pluschkell[10] attempted to develop a simulation model to describe the change in the nitrogen content of the metal in the BOF process. The authors predicted the change in nitrogen content during the blow by using a thermodynamic model. Deviations from equilibrium conditions due to kinetic limitations were considered in their model by introducing an efficiency parameter. The investigators arbitrarily selected an efficiency parameter as a correction factor for the deviation of the nitrogen content predicted by their thermodynamic

D.A. GOLDSTEIN, Research Engineer, is with the Homer Research Laboratory, Bethlehem Steel Corporation, Bethlehem, PA 18016. R.J. FRUEHAN, Professor, is with the Materials Science and Engineering Department Carnegie Mellon University, Pittsburgh, PA 15213.

Manuscript submitted August 20, 1998.

model from the nitrogen content normally found in actual steelmaking operations. It must be stressed that Kempken and Pluschkell's work is not a kinetic model; it is an equilibrium model with an arbitrary efficiency parameter that is adjustable. It is the purpose of the present investigation to develop a kinetic model that predicts the change of nitrogen content of steel during oxygen steelmaking.

II. MATHEMATICAL MODEL

A kinetic model has been developed to quantify the effects of process variables, such as carbon oxidation, nitrogen content in the hot metal, scrap, DRI, oxygen blown, and the effect of bottom stirring, on the nitrogen content of steel during OSM. The model has also been used to predict nitrogenization of steel in the converter. The model predicts the nitrogen content of steel at turndown. Other factors that affect the nitrogen content of steel, such as reblows, waiting periods and nitrogen pickup during tap, are not included in the model.

A. *Kinetic Model for the Nitrogen Reaction during Steelmaking*

In the BOF steelmaking operation, the rate of nitrogen pickup or removal is controlled by liquid-phase mass transfer of nitrogen in the metal and by the kinetics of the following reaction:

$$N_{2(gas)} = 2\underline{N} \qquad [1]$$

Several sequential mixed control models for the nitrogen reaction in liquid iron alloys have been developed by different investigators, and the details are given elsewhere.[7] In the present work, the change in nitrogen content of the metal during steelmaking is determined by using a steady-state model developed by Fruehan *et al.*[11] The rate equations used for these calculations are derived in a previous publication,[7] and the resultant expressions are shown subsequently:

$$\frac{k_a \cdot f_N^2}{K_N} \cdot [\text{pct N}_{surf}]^2 + \frac{m \cdot \rho}{100 \cdot MW_{N_2}} \cdot [\text{pct N}_{surf}] - \left(k_a \cdot P_{N_2} + \frac{m \cdot \rho}{100 \cdot MW_{N_2}} \cdot [\text{pct N}_{bulk}] \right) = 0 \qquad [2]$$

$$\left. \frac{d \text{ pct N}}{dt} \right|_{removed} = \frac{m \cdot A \cdot \rho}{W_m} \cdot (\text{pct N}_{surf} - \text{pct N}_{bulk}) \qquad [3]$$

$$\text{pct N}_{bulk}^{(i+1)} = \text{pct N}_{bulk}^{(i)} + \left(\left. \frac{d \text{ pct N}}{dt} \right|_{removed} \right) \cdot \Delta t + \sum_n \left(\left. \frac{d \text{ pct N}}{dt} \right|_{source}^{n} \right) \cdot \Delta t \qquad [4]$$

The change in nitrogen content during the blow is determined by solving Eqs. [2] through [4] simultaneously. The nitrogen content at the surface (pct N_{surf}) is obtained from Eq. [2], which depends on the nitrogen content in the bulk (pct N_{bulk}) and on the partial pressure of nitrogen in the gas phase (P_{N_2}). With the nitrogen contents at the surface and in the bulk, the rate of nitrogen removal from the metal is computed from Eq. [3]. Finally, the nitrogen content in the bulk of the metal is computed from Eq. [4], which depends on the rate of nitrogen removal calculated from Eq. [3] and from the rate of nitrogen pickup from different sources such as scrap, DRI, and bottom stirring.

The apparent rate constant, k_a, for the nitrogen reaction on the metal surface depends on the melt chemistry, in particular, on the activities of sulfur and oxygen at the gas-metal interface. Sulfur and oxygen are surface active in liquid iron alloys and block reaction sites for the formation or dissociation of the nitrogen molecule. The chemical rate constant for the nitrogen reaction with an iron alloy containing sulfur and oxygen is obtained from the rate constant on the bare iron surface (k_b) and from the activities of sulfur and oxygen at the gas metal interface (h_S and h_O), as shown in the following expression:[23]

$$k_a = \left(\frac{k_b}{1 + K_S \cdot h_S + K_O \cdot h_O} + k_r \right) \qquad [5]$$

The residual rate (k_r) will be neglected in the present study, since the sulfur contents in the metal are low and far from the residual rate phenomena for sulfur. Also, Fruehan and Martonik[12] did not observe the residual rate phenomena to occur for oxygen, even at very high oxygen contents. The temperature dependence of k_b and of the adsorption coefficients for sulfur and oxygen (K_S and K_O) are obtained from previous investigations and are outlined in Table I. Expressions used to determine the values of the equilibrium constant for Reaction [1], K_N, and for the activity coefficient of nitrogen (f_N) are also shown in Table I.

The change in temperature and melt chemistry during the blow are included in the model, in particular, the change in oxygen and sulfur contents of the metal that strongly affect the rate of the nitrogen reaction.

B. *Temperature Change during the Blow*

The change in the bath temperature during the blow is obtained from measurements made by previous investigators in a 50-metric-ton converter.[17] A correlation was developed from their experimental data (Eq. [11]) and used for the present calculations. The temperature of the slag-metal-gas emulsion is assumed to be 100 °C higher than that of the bath. These temperature profiles are assumed to be linear; however, a faster increase is expected at the beginning of the blow due to silicon oxidation. The actual temperature in any process depends on the specific operating conditions, and the variations in temperature from one process to another do not have significant effects on the model predictions.

$$T \text{ (in °C)} = 28 \cdot (\text{time in minutes}) + 1280 \qquad [11]$$

C. *Change in Melt Chemistry during the Blow*

Quantitative information of the change in melt chemistry during the blow is of primary importance for nitrogen removal calculations. In particular, it is important to know the silicon and carbon contents of the melt at any given time. Silicon oxidation occurs early in the blow to form SiO_2. The factors that control the rate of silicon oxidation depend on the amount of silicon in the bath. At high silicon levels, the rate is primarily controlled by the rate at which oxygen is supplied into the bath. At low silicon contents

Table I. Temperature and Composition Dependence for Model Parameters

Model Parameters	Expression	Reference
Rate on bare iron surface	$\log k_b = -\frac{6340}{T} - 1.38$ [6]	13
Adsorption coefficient for sulfur	$\log K_S = \frac{5874}{T} - 0.95$ [7]	14
Adsorption coefficient for oxygen	$\log K_O = \frac{11{,}370}{T} - 4.09$ [8]	15
Equilibrium constant	$\log K_N = -\frac{865.486}{T} - 5.747$ [9]	16
Activity coefficient	$\log f_N = e_N^C \cdot [\text{pct } C_{surf}]$ [10]	16

Table II. Determination of the Silicon Content during the Blow

Regime	Silicon Content	Expression	
(i) Oxygen flow rate control	pct Si > pct Si_{cr}	$\frac{d \text{ pct Si}}{dt} = -\frac{N_{O_2} \cdot MW_{Si} \cdot 100}{W_m}$	[12]
(ii) Mass-transfer control	pct Si < pct Si_{cr}	$\frac{d \text{ pct Si}}{dt} = -\frac{m_{Si} \cdot A \cdot \rho}{W_m} \cdot (\text{pct Si} - \text{pct Si}^e)$	[13]

Table III. Determination of the Bulk Carbon Content during the Blow

Regime	Carbon, Silicon	Expression	
(i) No carbon oxidation	pct C = 4.5 pct high silicon	pct C ≅ 4.5 pct	
(ii) Oxygen flow rate control	pct C > pct C_{cr} pct Si < 0.005 pct	$\frac{d \text{ pct C}}{dt} = \frac{N_{O_2} \cdot MW_c \cdot 100 \cdot (1 + F_{CO})}{W_m}$	[14]
(iii) Mass-transfer control	pct C < pct C_{cr} pct Si < 0.005 pct	$\frac{d \text{ pct C}}{dt} = \frac{m_c \cdot A \cdot \rho}{W_m} \cdot (\text{pct}C_{bulk})$	[15]

(<0.05 wt pct), the rate is primarily controlled by liquid-phase mass transfer of silicon to the reaction site. The rate expressions for both regimes are shown in Table II.

Carbon oxidation produces large amounts of CO, which removes nitrogen out of the melt and also affects the activities of sulfur and oxygen at the gas-metal interface. Carbon oxidation during the blow can be divided into three main regimes. During the first few minutes of the blow, silicon is being oxidized and no significant carbon oxidation occurs. In the second regime, the silicon content in the metal is very low (< 0.005 wt pct) and almost all the oxygen reacts with carbon. During this period, a gaseous product mixture of approximately 90 pct CO and 10 pct CO_2 is formed and a slag-metal-gas emulsion is produced. In this stage, the rate of decarburization is controlled by the flow rate of oxygen supplied. Finally, the last regime occurs at low carbon contents in the metal, where mass transfer of carbon to the gas-metal interface controls the rate of decarburization. The expressions needed to determine the change in the bulk content during these distinct stages are shown in Table III.

The critical carbon (pct C_{cr}) is the carbon content of the melt when the oxygen flow rate (Eq. [14]) equals the mass-transfer rate (Eq. [15]), resulting in

$$\text{pct } C_{cr} = \frac{N_{O_2} \cdot MW_C \cdot 100 \cdot (1 + F_{CO})}{m_c \cdot A \cdot \rho} \qquad [16]$$

It is also necessary to know the concentration of carbon at the gas-metal interface in order to determine the activity of surface-active elements such as oxygen and sulfur. The equations for the three regimes described previously are shown in Table IV. Because no emulsification occurs during silicon oxidation (first regime), a gas-metal interface is not present, and the carbon content at the surface is not relevant. In the second regime, the carbon content at the gas-metal interface is obtained by equating the mass-transfer rate to the oxygen-flow rate. In the final stage, when the decarburization rate is controlled by mass transfer, the carbon concentration at the surface is very low and assumed to be zero.

The change in the activity of oxygen at the gas-metal interface is determined by the model. At high carbon contents in the metal, above the critical carbon, the activity of oxygen at the interface is set by the C-CO equilibrium.[16] Below the critical carbon, the activity of oxygen at the interface is set by the Fe-FeO equilibrium.[16] This is because, at low carbon contents in the metal, the oxygen reacts with iron to form FeO. Table V outlines the equations needed to determine the activity of oxygen at the gas-metal interface. Both Eq. [19] and [21] result from the equilibrium of the C-CO and Fe-FeO reactions respectively. The temperature dependence of the equilibrium constant in Reaction [18] is small and was neglected for the model calculations.

Table IV. Determination of the Surface Carbon Content during the Blow

Regime	Expression
(i) No carbon oxidation	no emulsion during silicon oxidation; carbon at the surface is not relevant
(ii) Oxygen flow rate control	$\frac{m_c \cdot A \cdot \rho}{W_m} \cdot (\text{pct C}^{(j)}_{\text{bulk}} - \text{pct C}^{(j)}_{\text{surf}}) = \frac{\text{N}_{O2} \cdot MW_C \cdot 100 \cdot (1 + F_{CO})}{W_m}$ [17]
(iii) Mass-transfer control	$\text{pct C}_{\text{surf}} \approx 0$

Table V. Determination of the Activity of Oxygen at the Gas-Metal Interface

Regime	Expressions for Oxygen Activity	
pct C > pct C_{cr}	$C + O = CO_{(g)}$	[18]
	$h_O = \frac{0.002}{\text{pct C}_{\text{surf}}}$	[19]
pct C < pct C_{cr}	$FeO = Fe_{(l)} + O$	[20]
	$\log h_O = -\frac{6320}{T} + 2.734$	[21]

The activity of sulfur at the gas-metal interface is determined from Eq. [22]. The activity coefficient of sulfur is obtained from Eq. [23], and the sulfur content in the metal (pct S) is assumed to decrease linearly during the blow. (The initial sulfur content is the sulfur in the hot metal, assumed to be about 0.02 wt pct, and the final sulfur content is assumed to be 0.01 wt pct.[16])

$$h_S = f_S \cdot [\text{pct S}] \quad [22]$$

$$\log f_S = e^C_S \cdot [\text{pct C}_{\text{surf}}] \quad [23]$$

The mass-transfer parameter, *mA*, is determined by rearranging Eq. [16] to obtain Eq. [24]. It should be noted that Eq. [24] can be used to determine the mass-transfer parameter for different solutes, such as nitrogen and silicon in liquid iron, since their diffusion coefficients are similar.

$$m \cdot A = \frac{N_{O_2} \cdot MW_C \cdot 100 \cdot (1 + F_{CO})}{\text{pct C}_{cr} \cdot \rho} \quad [24]$$

For the model calculations, a critical carbon of 0.3 pct [18] is introduced into Eq. [24], and a volumetric mass-transfer parameter $\left(\frac{m \cdot A \cdot \rho}{W_m}\right)$ is computed as approximately 1.01 min^{-1} for an oxygen blow rate of 650 N m^3 min^{-1}.

The partial pressure of nitrogen in the gas phase is related to the mole fraction of nitrogen in the gas and to the total pressure. The total number of moles in the gas phase includes the moles of nitrogen removed from the melt into the gas, the moles of nitrogen in the oxygen present as an impurity, the moles of nitrogen from bottom stirring, the moles of CO and CO_2 produced from decarburization, and the moles of argon from bottom gas stirring. Thus, for a total pressure of 1 atm, the partial pressure of nitrogen can be determined from Eq. [25]. Expressions to compute the moles of nitrogen and CO in the gas phase are outlined in Tables VI and VII.

$$P_{N_2} = \frac{N^{\text{removed}}_{N_2} + N^{O}_{N_2} + N^{\text{stirring}}_{N_2}}{N^{\text{removed}}_{N_2} + N^{O}_{N_2} + N^{\text{stirring}}_{N_2} + N_{CO} + N^{\text{stirring}}_{Ar}} \quad [25]$$

D. *Nitrogen Pickup from Scrap and DRI*

Scrap and DRI are used as coolants during OSM. The rate of nitrogen pickup from scrap depends on the melting rate of scrap during steelmaking. Gaye *et al.*[19] developed and tested a mathematical model that predicts scrap dissolution in a converter. Their results indicate that light scrap, or slabs about 4-cm (1.5-in.) thick, melt early during the blow, whereas heavy scrap, or slabs about 14-cm (5.5-in.) thick, melt late in the blow. Their results are used in the present model to predict the effect of scrap size on the nitrogen content of the metal during the blow. The effect of scrap size on the nitrogen content of steel produced in the BOF is examined for two different cases. In the first case, it is assumed that 90 pct of the scrap charged into the furnace is heavy scrap (14-cm thick), and the remaining 10 pct is light scrap (4-cm thick). In the second case, 90 pct of the scrap charged is light scrap, and the remaining is heavy scrap.

The melting rate of heavy scrap during the blow is obtained from the work done by Gaye *et al.*[19] A correlation is obtained from their data and is used in the present calculations to predict the rate of nitrogen pickup from heavy scrap. The melting rate of light scrap is fast. For the model calculations, light scrap is assumed to melt linearly during the first 5 minutes of the blow. Direct reduced iron (DRI) can be used as a coolant in OSM instead of scrap. The DRI is known to melt quickly during steelmaking. In the model calculations, DRI is assumed to be charged early in the blow and melts linearly in 5 minutes. This assumption does not cause significant error in the model predictions because the amount of nitrogen in DRI is low.

E. *Nitrogen Pickup from Bottom Gas Stirring*

When nitrogen is used for bottom stirring, part of the nitrogen is absorbed into the melt as it rises through the bath, and the rest goes into the gas phase over the melt, increasing the partial pressure of nitrogen in the emulsion. When argon is used for stirring, it removes nitrogen from the melt as it rises through the bath and decreases the partial pressure of nitrogen in the gas phase over the melt. The rate of nitrogen absorption or desorption at the stirring site by the bottom injected gases is determined in a manner similar to that described previously for the emulsion. In brief, Eqs. [2] and [3] are used to determine the surface nitrogen and the rate at the stirring site, respectively. The resultant rate is introduced into Eq. [4] as a source term to calculate the nitrogen content in the bulk of the metal. The model calculations at the stirring site differ from the ones at the emulsion site in the following ways:

(1) The bath temperature is used at the stirring site instead of the emulsion temperature.
(2) The oxygen and sulfur activities at the gas-metal interface of the stirring site are computed from Eqs. [19] and [22]. At the stirring site, the bulk carbon content is used instead of the surface carbon concentration because no decarburization occurs at this site.

Table VI. Determination of the Moles of Nitrogen in the Gas Phase

Nitrogen removed from the melt into the gas phase	$\dot{N}_{N_2}^{\text{removed}} = \frac{1}{2} \cdot \left(\left. \frac{d \text{ pct N}}{dt} \right\vert_{\text{removed}} \right) \cdot \frac{W_m}{100 \cdot MW_{N_2}}$	[26]
Nitrogen impurity in the oxygen blown	$\dot{N}_{N_2}^{O} = \left(\frac{\text{vol pct } N_O}{.100} \right) \cdot \dot{N}_{O2}$	[27]
Nitrogen from bottom gas stirring	$\dot{N}_{N_2}^{\text{stirring}} = \frac{V_{N_2}^{\text{stirring}}}{0.0245} - \left(\left. \frac{d \text{ pct N}}{dt} \right\vert_{\text{stirring}} \cdot \frac{Wm}{100 \cdot MW_{N_2}} \right)$	[28]

Table VII. Determination of the Molar Flow Rate of Gas from Decarburization

Regime	Carbon, Silicon	Expressions	
(i) No carbon oxidation	pct C = 4.5 pct pct Si > pct Si_{cr}	$\dot{N}_{CO} \cong 0$ (no emulsification)	
(ii) Oxygen flow rate control	pct C > pct C_{cr} pct Si < 0.005 pct	$\dot{N}_{CO} = (1 + F_{CO}) \cdot \dot{N}_{O2}$	[29]
(iii) Mass-transfer control	pct C < pct C_{cr} pct Si < 0.005 pct	$\dot{N}_{CO} = \left(\frac{d \text{ pct C}}{dt} \right) \cdot \frac{W_m}{100 \cdot MW_C}$ or	[30]
		$\dot{N}_{CO} = \frac{m \cdot A \cdot \rho}{100 \cdot MW_C} \cdot (\text{pct } C_{bulk})$	[31]

(3) The partial pressure of nitrogen at the stirring site depends on the stirring gas used. If nitrogen is used for stirring, the partial pressure of nitrogen equals the atmospheric pressure affected by the ferrostatic head. If argon is used for stirring, the partial pressure of nitrogen is calculated from the following equation:

$$P_{N_2}^{\text{stirring site}} = \frac{\dot{N}_{N_2}^{\text{stirring site}}}{\dot{N}_{N_2}^{\text{stirring site}} + \dot{N}_{Ar}} \cdot P_T \qquad [32]$$

(4) At the stirring site, the mass-transfer parameter mA is different than at the emulsion. Extensive work has been done by several investigators to predict the behavior of gas jets in liquids. Abel and Fruehan[20] employed water modeling to investigate fluid flow and mass-transfer phenomena in large hot metal converters. Dimensionless analysis and regression analysis were used by Abel to develop empirical mass-transfer correlations to extrapolate his water modeling results to commercial bottom-blown processes. A liquid-gas bubble mass-transfer correlation (Eq. [33]), proposed by Abel and Fruehan,[20] is used to determine the mass-transfer parameter at the stirring site. This correlation predicts reasonable values of mA for the stirring gas in the present study. Using Eq. [33], the mass-transfer parameter ($m \cdot A \cdot \rho/W_m$) for the stirring site is computed to be 0.0046/min^{-1} for a gas flow rate of 10 N/m^3 min^{-1}.

$$m \cdot A = 8.383 \cdot 10^7 \cdot \left(\frac{D \cdot \rho_l^{0.36} \cdot \rho_g^{1.05} \cdot Q_{T,P}^{0.94} \cdot H_l^{0.34} \cdot (1 - \alpha)^{0.22}}{\sigma_{g-l}^{0.36} \cdot \Delta\rho_{g-l}^{1.05} \cdot d_b^{0.27}} \right) \qquad [33]$$

III. RESULTS AND DISCUSSION

The mixed control model described was solved for the case of a 200-metric-ton (220 ton) BOF charged with hot metal and scrap or DRI. The oxidation of carbon in the hot metal was achieved by oxygen blown at high flow rates from the top of the vessel. First, the model was used to predict the change in the nitrogen content of the metal for the base case described in Table VIII. Then the model was used to study the effects of several process variables on the bath nitrogen content. Figure 1 illustrates the change in melt chemistry during the blow in the converter. The changes in carbon and silicon contents in the metal are plotted as a function of time. The plotted lines clearly show the distinct regimes during carbon and silicon oxidation discussed previously. At the beginning of the blow, silicon was oxidized to silica and little carbon oxidation occurred. At lower silicon levels, carbon started to oxidize until a constant rate of decarburization was obtained. Finally, at low carbon levels, the rate of carbon removal was slowed by mass-transfer limitations.

Figure 2 shows the change in the activities of sulfur and oxygen at the gas-metal interface during the blow. The sulfur content of the metal was assumed to decrease linearly from 0.02 to 0.01 wt pct, and the activity of sulfur at the gas-metal interface was obtained by introducing the effect of carbon on the activity coefficient of sulfur. The change in the activity of oxygen at the gas-metal interface was obtained from thermodynamic calculations outlined in Table V. At high carbon contents in the metal, the oxygen activity at the gas-metal interface is set by the C-CO equilibrium. At low carbon contents, the decarburization efficiency is low, and the oxygen activity at the surface increases rapidly because it is set by the Fe-FeO equilibrium.

The amount of CO evolution from carbon oxidation during the blow was calculated and shown in Figure 3. Initially, CO evolution was low because silicon was being oxidized. Then at low silicon levels, CO evolution increased rapidly until it reached a constant value. Finally, it decreased when the level of carbon in the metal reached the critical carbon content of about 0.3 pct.

The chemical rate constant for the nitrogen reaction at the emulsion site was strongly affected by the change in the

Table VIII. Base Case for Nitrogen Control during OSM

BOF description	total weight of the metal (hot metal + coolant)	200-metric tonne (440,000 lbs)
	bath diameter	6 m (~20 ft)
	bath height (considering that one-third of the metal is in the emulsion in the blow)	1.4 m (~60 in.)
Oxygen injected (top lance blow)	flow rate	650 N m^3 min^{-1} (22,750 scfm) or 3.25 N m^3 min^{-1} $tonne^{-1}$
	nitrogen impurity	100 ppm
Chemistry of the hot metal	initial chemistry	carbon: 4.5 pct silicon: 0.6 pct sulfur: 0.02 pct nitrogen: 80 ppm
	final chemistry	carbon: 0.03 pct silicon: 0.002 pct sulfur: 0.01 pct
Coolants	scrap	amount charged: 20 pct of the total weight charged (40 tonne of scrap) nitrogen content: 50 ppm scrap size: 90 pct heavy scrap (slabs of 14-cm thick), and 10 pct light scrap (slabs of 4-cm thick)

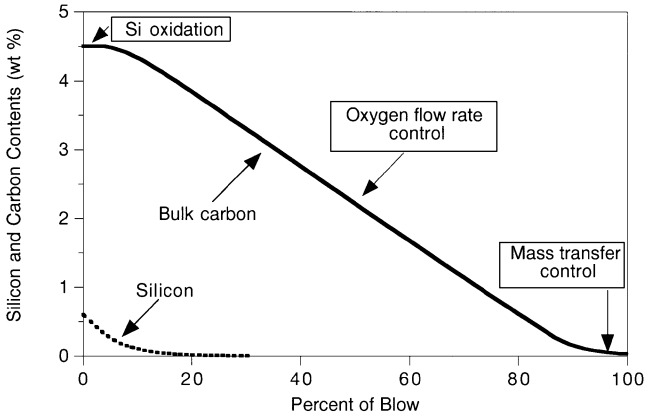

Fig. 1—Change in melt chemistry during the blow.

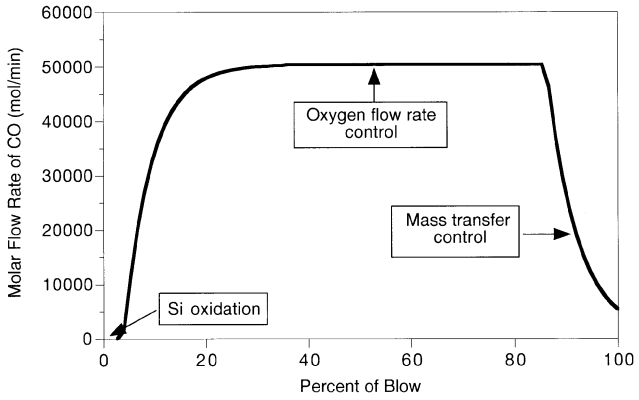

Fig. 3—Molar flow rate of CO during the blow.

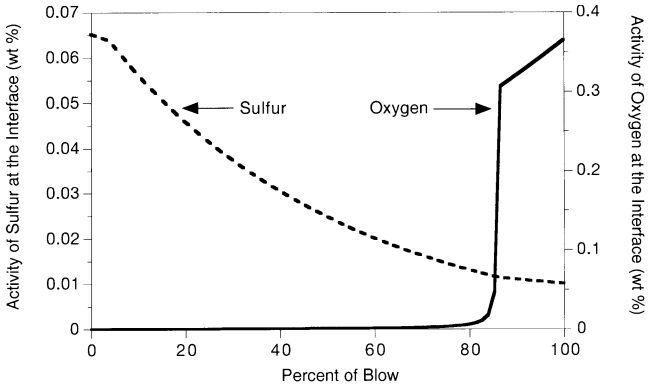

Fig. 2—Change in oxygen and sulfur activities at the gas-metal interface.

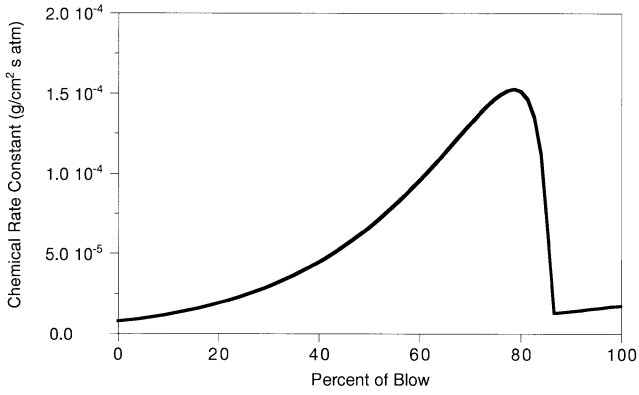

Fig. 4—Change in the chemical rate constant for nitrogen at the emulsion.

activities of oxygen and sulfur at the interface and by the change in temperature during the blow. Figure 4 presents the change in the apparent chemical rate constant for nitrogen during the process. At the beginning of the blow, the rate constant was low, because the temperature was relatively low and the activity of sulfur at the interface was high. As the temperature increased and the activity of sulfur decreased, the rate constant increased. Finally, at the end of the blow, the activity of oxygen at the interface increased

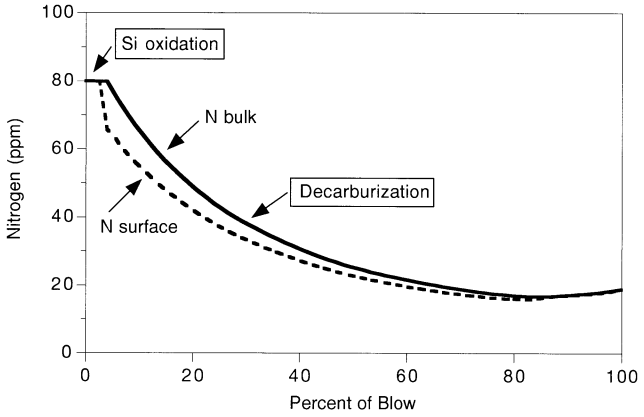

Fig. 5—Bulk and surface nitrogen concentrations during the blow.

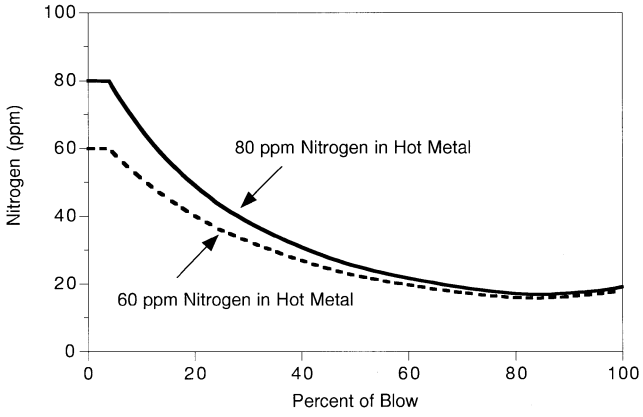

Fig. 6—Effect of nitrogen content in the hot metal on the bath nitrogen content.

(Figure 2), and consequently, the rate constant dropped significantly. Also shown in Figure 4 is a small increase in the rate during the last few minutes of the blow. This was due to the increase in temperature that occurred in this stage of the blow. However, this effect was small, and the high activity of oxygen at the reaction site governed the chemical rate constant.

Figure 5 shows the change in the nitrogen concentrations in the bulk and surface during the blow. The results appear to indicate that the rate of nitrogen removal in the emulsion is mostly controlled by chemical kinetics. This is because the nitrogen contents in the bulk and the surface were similar, indicating that liquid mass transfer of nitrogen was fast.

Figure 5 also shows an increase in the nitrogen content in the metal at the end of the blow due to heavy scrap melting late in the process. The nitrogen released from scrap remained in the metal because little CO was produced at this time and also because the activity of oxygen at the interface was high late in the blow.

The results shown so far are for the base case described in Table VIII. In the following sections, the model is used to predict the effect of different operational parameters on the change in bath nitrogen content. It should be noted that in the analysis of a given parameter, only that parameter is varied and the rest will remain as specified by Table VIII.

A. *Effect of Nitrogen Content in the Hot Metal*

The effect of the nitrogen present in the hot metal on the final nitrogen content of steel is shown in Figure 6. The model was solved for two different nitrogen concentrations in the hot metal (60 and 80 ppm). From the results, and in agreement with other investigators, it is observed that an increase of nitrogen in the hot metal of about 20 ppm will increase the nitrogen content of steel by only 1 or 2 ppm.[3]

B. *Effect of Sulfur Content in the Hot Metal*

The sulfur content in the hot metal has an important effect on the bath nitrogen content. Sulfur retards the rate of nitrogen removal. When sulfur in the hot metal is decreased from 0.02 to 0.004 wt pct, more nitrogen is removed early in the blow (Figure 7).

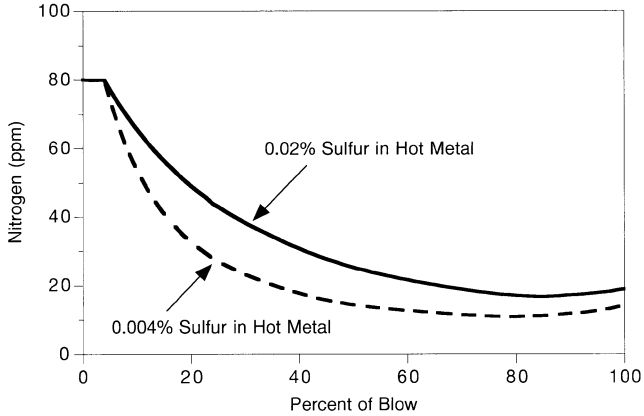

Fig. 7—Effect of sulfur content in the hot metal on the bath nitrogen content.

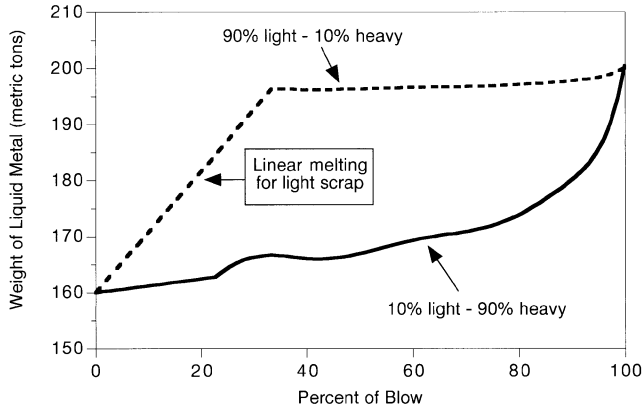

Fig. 8—Weight change of the metal bath from scrap melting.

C. *Effect of Coolants Such as Scrap and DRI*

The effect of scrap size on the bath nitrogen, and the effect of using scrap *vs* low-nitrogen scrap alternatives such as DRI, was investigated with the model. The amount of coolants used, specified as a percent of the total metallic charge into the furnace, was 20 pct for scrap and 15 pct for DRI. These percentages are usually determined from mass and energy balance calculations for a given heat, but in this investigation, they were obtained from the literature.[16]

As shown in Figure 8, heavy scrap melts late in the

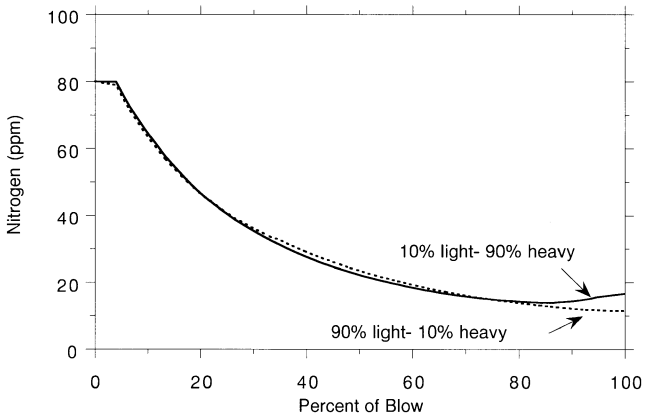

Fig. 9—Effect of scrap size on the bath nitrogen content.

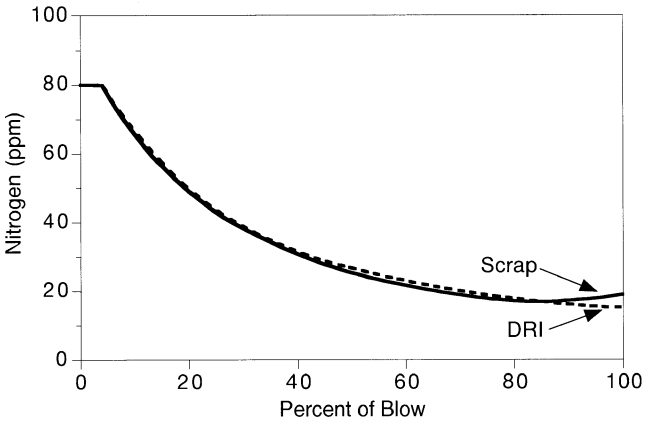

Fig. 10—Effect of scrap and DRI on the bath nitrogen content.

blow,[19] and because little CO is produced in this stage, the bath nitrogen content increases. On the other hand, light scrap melts quickly at the beginning of the blow, and the nitrogen from scrap absorbed into the bath is removed during decarburization. The model calculations indicate that the turndown nitrogen content produced using 90 pct heavy scrap is about 7 ppm higher than when 90 pct light scrap is used, as seen in Figure 9.

A comparison of the effects of scrap and DRI on the bath nitrogen content is shown in Figure 10. For the case of scrap, 40 metric tons were charged into the converter, of which 90 pct was heavy scrap. For the case of DRI, only 30 metric tons were charged into the converter. When DRI was used for cooling, the final nitrogen content of steel was lower than when heavy scrap was used for cooling. This is because DRI contains lower nitrogen levels than scrap, and DRI melts earlier in the blow, as shown in Figure 11.

D. *Effect of Nitrogen Present in the Oxygen Blown*

Figure 12 shows that nitrogen present as an impurity in the oxygen blown increases the nitrogen partial pressure in the gas phase of the emulsion. This is especially true at the end of the blow because the amount of CO that dilutes the nitrogen in the gas phase is low. The model predictions shown in Figure 13 indicate that an increase in the nitrogen

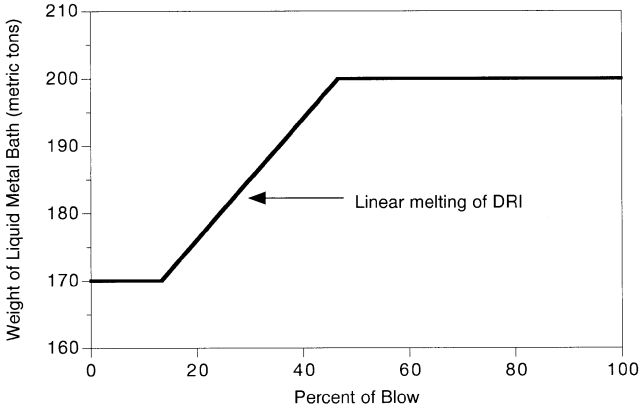

Fig. 11—Weight change of the metal from DRI additions.

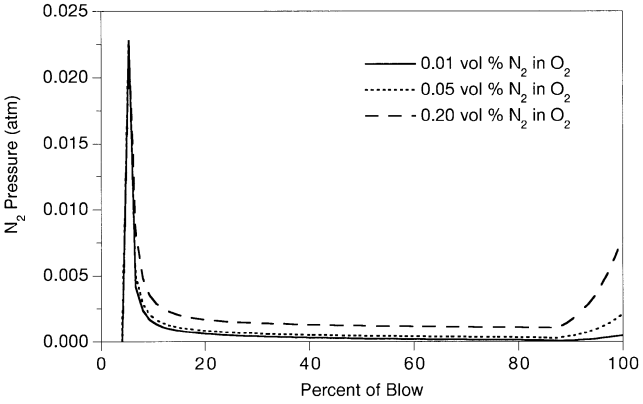

Fig. 12—Effect of nitrogen impurity on the partial pressure of nitrogen in the gas.

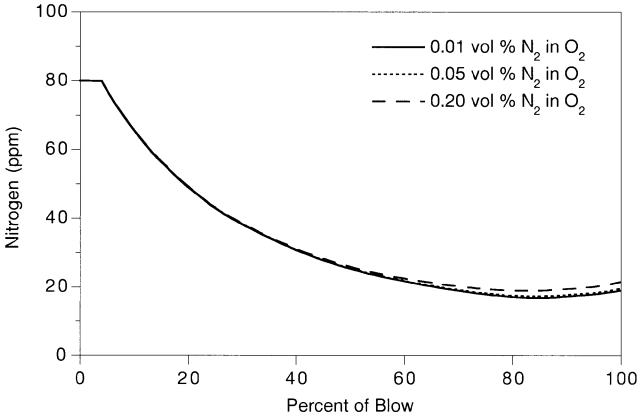

Fig. 13—Effect of nitrogen impurity in the oxygen on the bath nitrogen content.

impurity from 100 to 2000 ppm will increase the bath nitrogen content by approximately 3 ppm. This small increase in nitrogen pickup into the melt indicates that levels of nitrogen in the oxygen below 2000 ppm do not increase the partial pressure of nitrogen in the emulsion enough to cause significant nitrogen pickup. Also, the high activity of oxygen at the interface late in the blow inhibits nitrogen pickup from the oxygen supplied late in the blow.

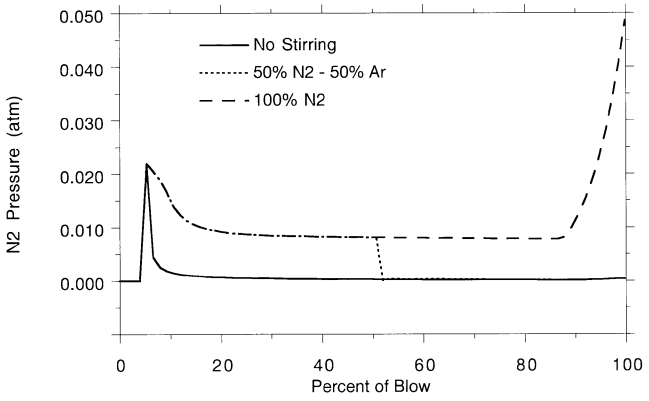

Fig. 14—Effect of bottom gas stirring on the partial pressure of nitrogen in the gas phase of the emulsion.

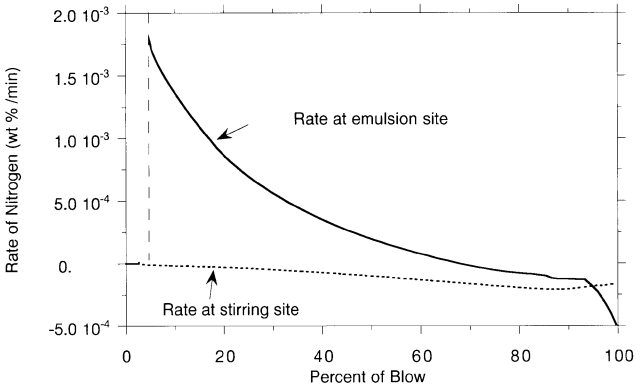

Fig. 15—Rate of nitrogen removal and pickup during combined gas blowing with nitrogen.

E. *Effect of Bottom Stirring*

Stirring in the converter is usually done with gases such as nitrogen and argon. During the analysis of bottom stirring, three different cases were considered: one in which nitrogen gas was used for the entire stirring period, another in which nitrogen was used during the first half of the stirring period and argon for the second half, and one with no bottom stirring. The gas flow rate used for the model calculations was 10 N m^3 min^{-1} (350 scfm) or 0.05 N m^3 min^{-1} $tonne^{-1}$. In the model calculations, two effects were considered: the change in the nitrogen pressure in the emulsion and the pickup or removal of nitrogen in the metal as nitrogen or argon rose through the bath. Figure 14 shows the effect of bottom stirring on the nitrogen partial pressure in the emulsion. When nitrogen was used as a stirring gas, high partial pressures of nitrogen were developed in the gas phase of the emulsion, which caused nitrogen pickup into the metal. This was especially true at the end of the blow.

Figure 15 compares the rate of the nitrogen reaction at the emulsion site with the rate of the nitrogen reaction at the stirring site as nitrogen gas rose through the bath. In this figure, a negative rate indicates that nitrogen was absorbed into the metal; a positive rate indicates that nitrogen was removed from the metal. The results shown in this figure assume that nitrogen was used for stirring during all of the blow. Because the partial pressure of nitrogen in the emulsion increased at the end of the blow (Figure 14), there was a transfer of nitrogen from the gas back into the metal. This is shown as a negative rate in Figure 15. This transfer, in combination with the nitrogen absorbed at the stirring site, resulted in high final nitrogen levels when nitrogen was used for stirring late in the blow. Figure 16 shows the change of nitrogen content in the melt due to stirring. The results show that when nitrogen was used for the entire stirring time, the final nitrogen content increased by 25 ppm. Switching from nitrogen to argon at the midpoint of the blow produced lower turndown nitrogen levels. Figure 15 also shows that the rate of nitrogen pickup into the metal from the rising nitrogen gas was small compared with the rate of nitrogen pickup into the metal from the emulsion at the end of the blow. Therefore, for typical flow rates of nitrogen used for stirring during OSM, most of the increase in nitrogen (Figure 16) was due to the increase in the nitrogen partial pressure at the emulsion site.

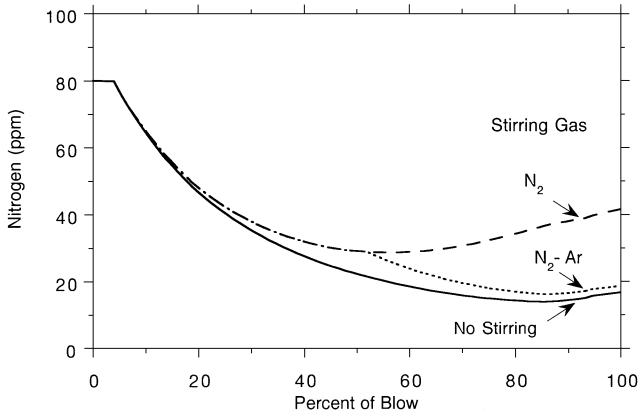

Fig. 16—Effect of bottom gas stirring on the bath nitrogen content.

The model calculations were compared to plant data from trials done at the Burns Harbor plant of Bethlehem Steel Corporation.[22] During these trials, nitrogen used for bottom stirring was replaced with argon at different percentages of completion of the oxygen blow. For each change from nitrogen to argon, turndown nitrogen levels were measured; their distributions are plotted in Figure 17. The mean nitrogen content was computed for each distribution, and is shown in each plot as the actual nitrogen level. A calculated nitrogen level was also obtained by introducing the process parameters used during these trials into the current model. Figure 17 shows that the calculated nitrogen level obtained from the model is in good agreement with the mean or actual nitrogen level obtained from the plant data. This establishes the model as a useful tool to predict the turndown nitrogen content for different mixed blowing conditions.

F. *Nitrogenization of Steel in the BOF*

Nitrogenization of steel in the converter can be carried out by injecting nitrogen through the main lance with the oxygen during the blow. Boting and Kreyger[2] successfully found this to be a reproducible solution for the production of high nitrogen steels in the converter. They were able to produce steels containing up to 120 ppm in nitrogen by supplying the nitrogen gas with the oxygen at the end of the blow. The plant trials were carried out in a 300-tonne converter at Hoogovens IJmuiden BV. Nitrogen was injected

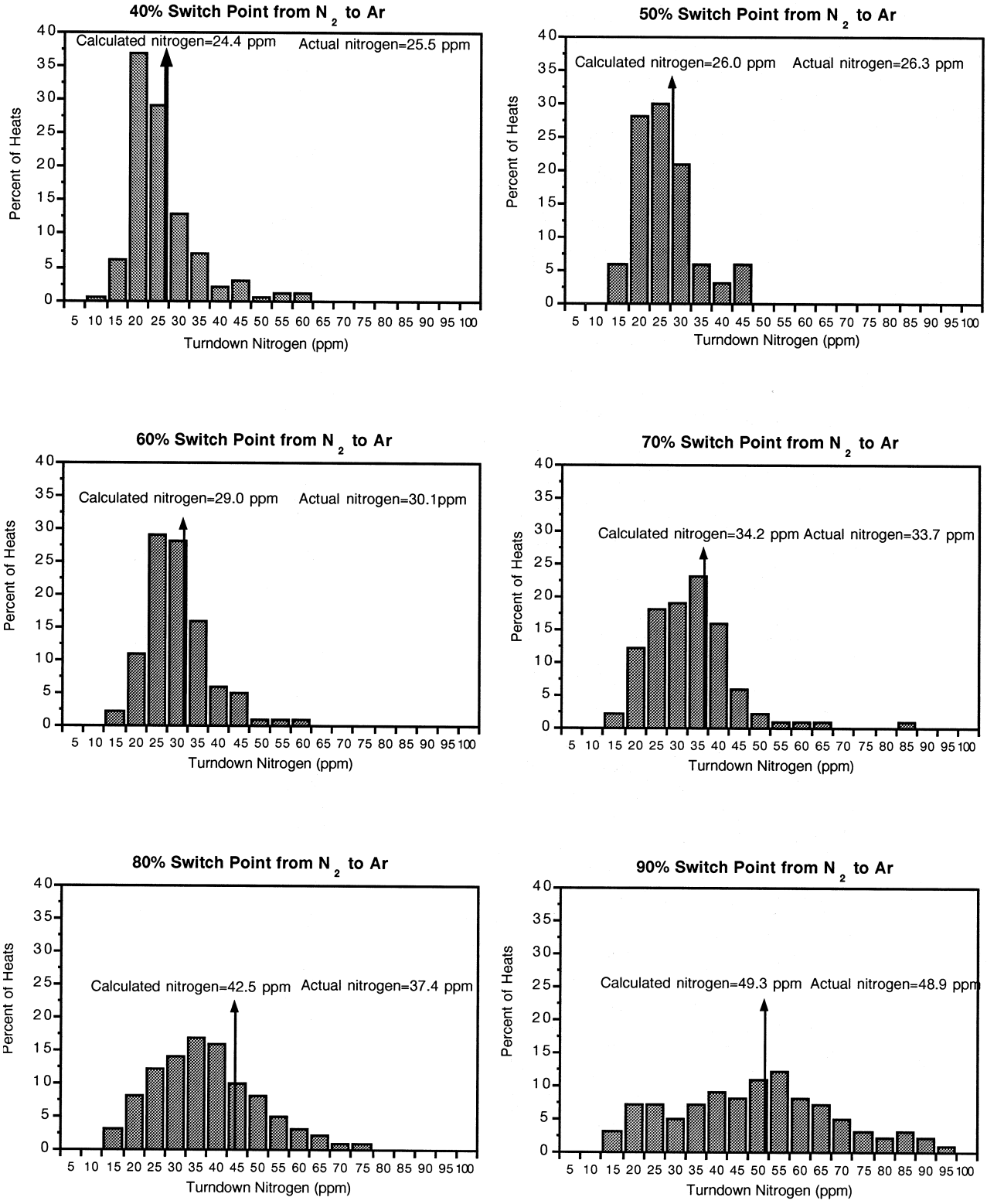

Fig. 17—Comparison of model predictions to plant data.

at flow rates between 30 and 100 N m^3 min^{-1} for about 3 to 11 minutes. The authors developed a practical relationship (Eq. [34]) that permits the selection of adequate flow rates and injection times to meet the desired nitrogen content:

$$\text{N (ppm)} = 17.2 + 3.6 \cdot \sqrt{Q_{N_2}} \qquad [34]$$

where Q_{N_2} is the volume of nitrogen injected, which is obtained from the nitrogen flow rate and the injection time.

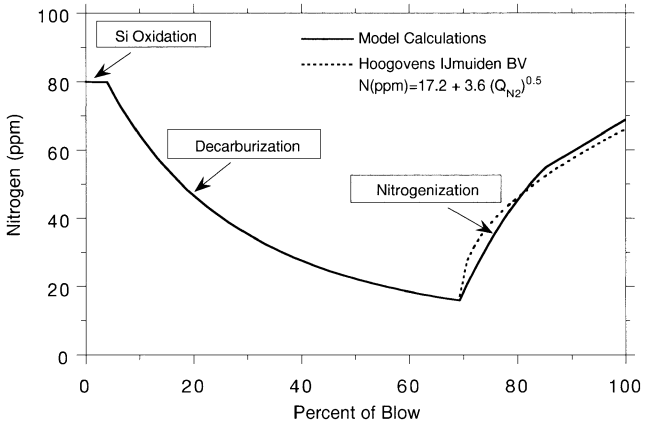

Fig. 18—Nitrogenization of steel in the converter.

The dashed line in Figure 18 represents Hoogovens[2] prediction of nitrogen pickup into the steel when 40 N m^3 min^{-1} of nitrogen is injected with the oxygen flow during the last 5 minutes of the blow. The parameters used by the investigators were introduced into the present model and are also plotted in Figure 18. The model calculations predict an increase in nitrogen content of steel similar to that obtained in the plant trials.

IV. CONCLUSIONS

A kinetic model was developed that provides a quantitative understanding of how different operational parameters affect the final nitrogen content of steel during OSM. The model predicts the minimum final nitrogen levels of steel that can be produced. This is because operational factors such as reblows, waiting periods, and tapping, that affect the nitrogen content of steel, are not included in the model. The results from the model calculations indicate the following.

1. Nitrogen is mostly removed from the melt at high carbon contents (>0.3 wt pct C) by the CO produced during decarburization. At low carbon contents (<0.3 wt pct C), it is difficult to remove the nitrogen from the melt because the decarburization efficiency is low. Consequently, little CO is produced and the activity of oxygen at the gas-metal interface is high, reducing the nitrogen reaction rate.
2. Nitrogen in the hot metal does not have a significant effect on the final nitrogen content of steel, because the nitrogen in the hot metal is removed during decarburization. Sulfur in the hot metal does appear to affect the rate of nitrogen removal during decarburization.
3. Nitrogen in scrap can increase the final nitrogen content of steel, particularly if scrap melts late in the process. Therefore, heavy scrap must be avoided to produce low nitrogen steels. The use of high-quality light scrap or scrap alternatives, such as DRI and iron ore, for cooling is required to produced ultra low nitrogen steels.
4. Nitrogen impurity levels in the oxygen must be kept below about 0.2 vol pct to avoid excessive nitrogen pickup into the bath. To produce very low nitrogen steels, less than 0.01 vol pct of nitrogen in the oxygen is recommended.
5. Nitrogen used for bottom stirring increases the final nitrogen content of steel if it is used late in the blow. Reasonably low turndown nitrogen levels are achieved by switching from nitrogen to argon at about 50 pct of the blow.
6. Nitrogen alloying in the BOF by injecting nitrogen with the oxygen late in the blow is predicted with the present model. The model determines the selection of the necessary flow rates and nitrogen injection times to meet the desired final nitrogen content. The model calculations agree well with the experimental trials carried out at Hoogovens Ijmuiden.

ACKNOWLEDGMENTS

The authors acknowledge the Center for Iron and Steelmaking Research (CISR) and its member companies for the funding of this research and for their helpful discussions that gave a practical meaning to our investigation. The authors also thank Professor Alan Cramb, Dr. Michael Byrne, and Dr. Bahri Ozturk for their invaluable comments.

LIST OF SYMBOLS

A	gas-liquid metal interfacial area (cm^2)
a	gas holdup ($a = 0.05$)
D	diffusivity of nitrogen ($5 \cdot 10^{-5}$ cm^2 s^{-1})
d_b	bath diameter (cm)
e_N^C	interaction coefficient ($e_N^C = 0.13$)[21]
e_S^C	interaction coefficient ($e_S^C = 0.114$)[21]
F_{CO}	fraction of CO ($F_{CO} = 0.9$)
f_N	activity coefficient for nitrogen
f_S	activity coefficient for sulfur
h_S	activity of sulfur (wt pct)
h_O	activity of oxygen (wt pct)
H_l	bath height (cm)
j	time increment
k_a	rate constant in mol cm^{-2} s^{-1} atm^{-1}
k_b	rate constant in mol cm^{-2} s^{-1} atm^{-1}
k_r	rate constant in mol cm^{-2} s^{-1} atm^{-1}
K_S	adsorption coefficient for sulfur
K_O	adsorption coefficient for oxygen
K_N	equilibrium constant for Reaction [1]
m	mass-transfer coefficient for nitrogen (cm s^{-1})
m_C	mass-transfer coefficient for carbon (cm s^{-1})
m_{Si}	mass-transfer coefficient for silicon (cm s^{-1})
MW_C	molecular weight of carbon
MW_{N_2}	molecular weight of nitrogen
MW_{Si}	molecular weight of silicon
n	N_2 sources: scrap, DRI, nitrogen stirring
N_{O_2}	molar flow rate of O_2 (mol min^{-1})
N_{CO}	flow rate of decarburized gases (mol min^{-1})
$N_{N_2}^{removed}$	nitrogen removed (mol min^{-1})
$N_{N_2}^{O}$	nitrogen in the oxygen (mol min^{-1})
$N_{N_2}^{stirring}$	nitrogen from stirring (mol min^{-1})
$N_{Ar}^{stirring}$	argon from stirring (mol min^{-1})
P_T	atmospheric pressure (1 atm)
P_{N_2}	partial pressure of N_2 in the gas (atm)
$Q_{T,P}$	flow rate at T, P (cm^3 s^{-1})
Q_{N_2}	N_2 alloying ($Q_{N_2} = V_{N_2} \cdot t$) (N m^3)

T	temperature in Kelvin
$V_{N_2}^{stirring}$	flow rate of N_2 stirring (N m^3 min^{-1})
V_{N_2}	flow rate of N_2 alloying (N m^3 min^{-1})
vol pct N_{oxygen}	N_2 in the oxygen (vol pct)
W_m	weight of the melt (g)
pct C_{bulk}	carbon content in bulk (wt pct)
pct C_{surf}	carbon content at surface (wt pct)
pct N_{bulk}	nitrogen content in bulk (wt pct)
pct N_{surf}	nitrogen content at surface (wt pct)
pct S	sulfur content in the metal (wt pct)
pct Si_{cr}	critical silicon content (wt pct)
pct Si^e	final silicon (wt pct) (pct $Si^e = 0.002$)
σ_{g-l}	interfacial tension between liquid iron and gas (1760 dyn cm^{-1})
ρ	density of liquid iron (g cm^{-3})
ρ_g	density of the gas (g cm^{-3})
$\Delta\rho_{g-l}$	difference in densities (g cm^{-3})

REFERENCES

1. "Nitrogen Control in Electric Furnace Steelmaking," EPRI Report No. TR-101600, EPRI, Pleasant Hills CA, 1992.
2. P.G. Boting and P.J. Kreyger: *Steelmaking Conf. Proc.*, ISS, Warrendale, PA, 1978, vol. 61 pp. 362-68.
3. C. Marique, E. Beyne, and A. Palmaers: *Ironmaking and Steelmaking*, 1988, vol. 15, pp. 38-42.
4. L.M. Keilman: "Literature Survey on Nitrogen Control and Removal from Liquid Steel," AISI Metallurgical Subcommittee on Strand Casting, Inland Steel Industries, Inc., August 31, 1989, pp. 12-14.
5. J. Thomas, C. Scheid, and G. Geiger: *Electric Furnace Conf. Proc.*, ISS, Warrendale, PA, 1992, pp. 263-85.
6. L. Lifka, and Q.R. Skrabec: *I&SM*, 1984, Nov., pp. 32-36.
7. D.A. Goldstein, R.J. Fruehan, and B. Ozturk: *Trans. ISS, I&SM*, 1999, Feb., pp. 47-61.
8. P.C. Glaws and R.J. Fruehan: *Metall. Trans. B*, 1985, vol. 16B, pp. 551-59.
9. P.C. Glaws, G.J.W. Kor, and R.V. Fryan: *Electric Furnace Conf. Proc.*, ISS, Warrendale, PA, 1989, pp. 383-93.
10. J. Kempken and W. Pluschkell: *Stahl Eisen.*, 1995, vol. 115(8), pp. 67-73.
11. R.J. Fruehan, B. Lally, and P.C. Glaws: *I&SM*, 1987, Apr., pp. 31-36.
12. R.J. Fruehan and L.J. Martonik: *Metall. Trans. B*, 1980, vol. 11B, pp. 615-21.
13. M. Byrne and G.R. Belton: *Metall. Trans. B*, 1983, vol. 14B, pp. 441-49.
14. A.W. Cramb and I. Jimbo: *Steel Res.*, 1989, vol. 60, pp. 157-65.
15. A. Cramb and G.R Belton: *Metall. Trans. B*, 1981, vol. 12B, pp. 699-704.
16. *BOF Steelmaking*, R.D. Pehlke, W.F. Porter, R.F. Urban, and J.M. Gaines, eds., ISS-AIME, Warrendale, PA, 1977, vol. 2.
17. A. Masui, K. Yamada, and K. Takahashi: *McMaster Symp.*, 1976, May, pp. 1-31.
18. B. Deo and R. Boom: *Fundamentals of Steelmaking Metallurgy*, Prentice-Hall International, 1993, p. 194.
19. H. Gaye, M. Wanin, P. Gugliermina, and Ph. Schittly: *Steelmaking Conf. Proc.*, ISS, 1985, vol. 68 p. 91; *Proc. 6th Int. Iron and Steel Congress*, ISIJ, Nagoya, 1990, p. 11.
20. C. Abel and R.J. Fruehan: *Trans. ISS, I&SM*, 1995, Aug., pp. 49-64.
21. G.K. Sigworth and J.F. Elliott: *Met. Sci.*, 1974, vol. 8, pp. 298-310.
22. K.L. Chen and R.C. Novak: Burns Harbor Plant of Bethlehem Steel Corporation, Bethlehem, PA, 1995. [unpublished work]
23. G.R. Belton: *Can. Metall. Q.*, 1982, vol. 21 (2), pp. 137-43.